The Combined Effect of Modulator Imbalances and Amplifier Nonlinearity on the Performance of Offset Quadrature-Phase-Shift-Keyed (OQPSK) Systems

H. Tsou[1]

Imbalances from imperfect phase modulators can cause distorted signal constellations and interfering tone signals at the carrier frequency in phase-modulated communication systems. The rendered imperfection in the modulated signal inevitably degrades the receiver's carrier-tracking performance and, for quadrature-phase-shift-keyed (QPSK) systems in particular, causes cross-talk between the in-phase and quadrature-phase channels. Previous studies have analyzed the impact from the amplitude and phase imbalances on an offset QPSK (OQPSK) communication system with the assumption of a linear channel. This article extends such efforts by including a fully saturated radio-frequency (RF) amplifier in the analytical model. Both carrier-suppression level and bit-error performance are addressed in this article, showing that the amplifier nonlinearity greatly alleviates the impact from modulator imbalances. With current Consultative Committee for Space Data Systems (CCSDS) recommendations of a 2-deg-maximum permissible phase imbalance and a 0.2-dB-maximum permissible amplitude imbalance, a 34-dB or more carrier suppression and a system degradation of 0.27 dB or less at an uncoded bit-error probability of 10^{-4} are achievable when the OQPSK system is operated in a reasonable loop signal-to-noise ratio (SNR) region. These results are 9-dB better in terms of carrier suppression and 0.6-dB better in terms of system degradation than those with linear amplifiers at the aforementioned bit-error probability.

I. Introduction

Imbalances from imperfect phase modulators can cause distorted signal constellations and spurious carrier signals in phase-modulated communication systems. The rendered imperfection in the modulated signal inevitably degrades the receiver's carrier-tracking performance and, for quadrature-phase-shift-keyed (QPSK) systems in particular, causes cross-talk between the in-phase (I) and quadrature-phase (Q) channels. Moreover, the presence of a spurious carrier signal raises the concern of a spectral line exceeding the power-flux density limit on the Earth's surface for space applications.

A previous article [1] analyzed the impact from the amplitude and phase imbalances on the offset QPSK (OQPSK) system with the assumption of a linear channel and an imperfect balanced modulator model. The balanced modulator [2], which comprises two amplitude-modulation (AM) modules, is widely

[1] Communications Systems and Research Section.

used in phase-modulated communication systems. However, in practice, the balance between these AM modules is difficult to maintain perfectly, resulting in amplitude and phase imbalances in the modulated signal when such an imperfect modulator is used to modulate data directly onto the radio-frequency (RF) carrier.

This article extends the previous effort to nonlinear channels by including a fully saturated RF amplifier in the analytical model. It is assumed that, when no modulator imbalance exists, each OQPSK symbol is comprised of two independent information bits of equal bit rate and energy. The modulator imbalances, including both the interchannel and the intrachannel amplitude and phase imbalances, are specified by using the same balanced modulator model as the one used before. The resulting imperfectly modulated OQPSK signal first is passed through a highly saturated RF amplifier modeled by a bandpass hard limiter and then coherently demodulated by using the carrier reference derived from a modified $IQ(Q^2 - I^2)$-type QPSK carrier-tracking loop.

Section II describes the system model, including the imperfect OQPSK modulator and the bandpass hard limiter. The combined effects of modulator imbalances and amplifier nonlinearity on the carrier-suppression level and the irreducible carrier-tracking error are discussed in Sections III and IV. The bit-error-rate (BER) performance for various combinations of amplitude and phase imbalances within the maximum permissible imbalance figures currently recommended by the Consultative Committee for Space Data Systems (CCSDS) [3] are evaluated in Section V, followed by a conclusion in Section VI summarizing the worst-case carrier-suppression level and BER performance expected with the recommended maximum permissible modulator imbalances. Finally, alternative models of OQPSK modulator imbalances and their relationships with the balanced modulator model are included in the Appendix.

II. System Model

The block diagram of an OQPSK transmitter implemented with two balanced modulators, each consisting of two AM modules, followed by a nonlinear RF amplifier modeled by a bandpass hard limiter is shown in Fig.1. For each balanced modulator, the equally probable, nonreturn-to-zero, binary data are fed into its two AM modules, one of them receiving the data stream with inverted polarity. For perfectly balanced AM modules, the AM signals subtract to form a binary-phase-shift-keyed (BPSK) signal with the unmodulated carrier completely suppressed. However, with the presence of modulator imbalances, the modulated OQPSK signal becomes

$$S_o(t) = \sqrt{P}[(\alpha_1 \cos\omega_c t + \delta_1 \sin\omega_c t) + m_1(t)(\beta_1 \cos\omega_c t - \gamma_1 \sin\omega_c t)]$$

$$+ \sqrt{P}\left[(\alpha_2 \sin\omega_c t - \gamma_2 \cos\omega_c t) + m_2\left(t - \frac{T_s}{2}\right)(\beta_2 \sin\omega_c t + \gamma_2 \cos\omega_c t)\right] \tag{1}$$

or, equivalently,

$$S_o(t) = \sqrt{P}\left[\alpha_1 + \beta_1 m_1(t) - \gamma_2\left(1 - m_2\left[t - \frac{T_s}{2}\right]\right)\right]\cos\omega_c t$$

$$+ \sqrt{P}\left[\alpha_2 + \beta_2 m_2\left(t - \frac{T_s}{2}\right) + \delta_1 - \gamma_1 m_1(t)\right]\sin\omega_c t \tag{2}$$

where P is twice the power found in the I-channel;[2] T_s is the symbol duration; $m_1(t)$ and $m_2(t)$ are binary data for the I-channel and the Q-channel, respectively; and the coefficients are defined as follows:

[2] It also is designated as the nominal total power for both channels. The actual combined power is $P([1+\Gamma^2]/2) \leq P$, with the assumption that the Q-to-I power ratio is $\Gamma \leq 1$.

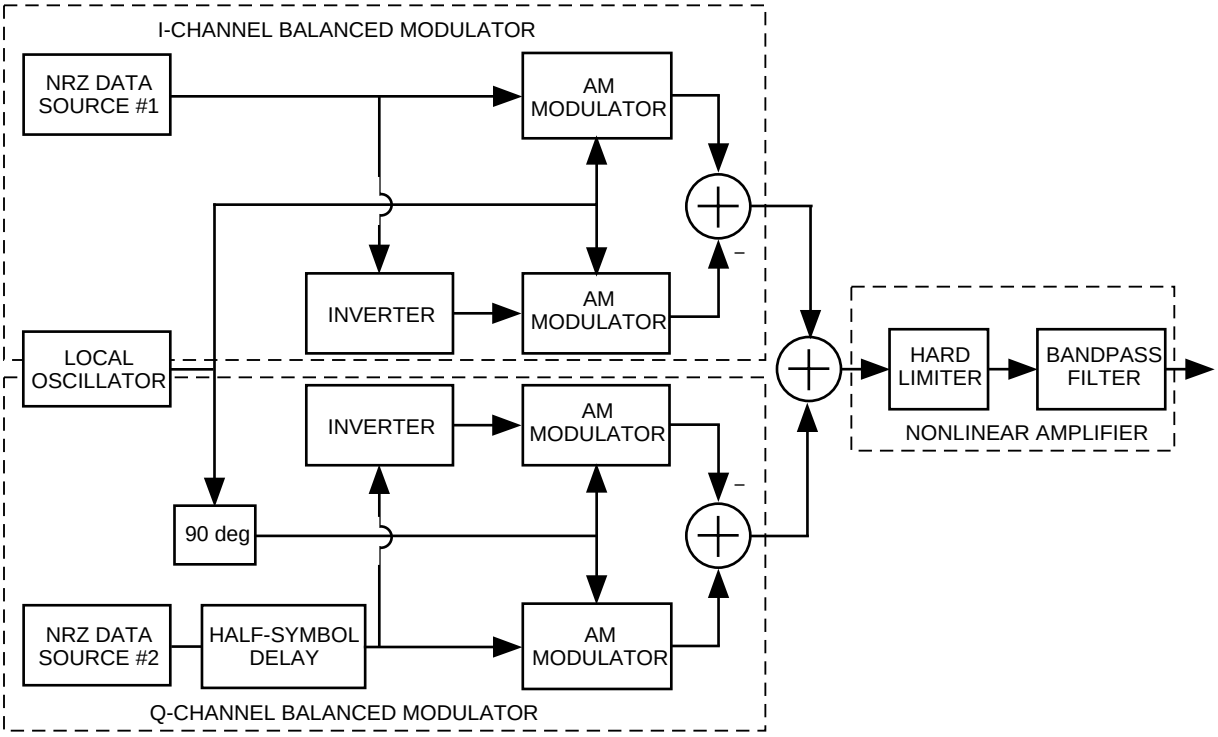

Fig. 1. The OQPSK transmitter model.

$$
\left.
\begin{aligned}
\alpha_1 &= \frac{(1-\Gamma_1\cos\Delta\theta_1)\cos\Delta\theta + \Gamma_1\sin\Delta\theta_1\sin\Delta\theta}{2} \\
\alpha_2 &= \Gamma\left(\frac{1-\Gamma_2\cos\Delta\theta_2}{2}\right) \\
\beta_1 &= \frac{(1+\Gamma_1\cos\Delta\theta_1)\cos\Delta\theta - \Gamma_1\sin\Delta\theta_1\sin\Delta\theta}{2} \\
\beta_2 &= \Gamma\left(\frac{1+\Gamma_2\cos\Delta\theta_2}{2}\right) \\
\gamma_1 &= \frac{(1+\Gamma_1\cos\Delta\theta_1)\sin\Delta\theta + \Gamma_1\sin\Delta\theta_1\cos\Delta\theta}{2} \\
\gamma_2 &= \Gamma\left(\frac{\Gamma_2\sin\Delta\theta_2}{2}\right) \\
\delta_1 &= \frac{-(1-\Gamma_1\cos\Delta\theta_1)\sin\Delta\theta + \Gamma_1\sin\Delta\theta_1\cos\Delta\theta}{2}
\end{aligned}
\right\} \qquad (3)
$$

where

$\Gamma =$ the interchannel amplitude imbalance or, equivalently, the square root of the Q-to-I power ratio between channels

$\Gamma_1, \Gamma_2 =$ the amplitude imbalances within each of the I-channel and Q-channel balanced modulators, respectively

$\Delta\theta =$ the interchannel phase error defined as the phase deviation from the ideal 90-deg separation between the I-channel and the Q-channel

$\Delta\theta_1, \Delta\theta_2 =$ the phase imbalances within each of the I-channel and Q-channel balanced modulators, respectively

Both the spurious carrier components and the cross-talk between channels are clearly shown in Eq. (2). Figure 2(a) shows the phasor representation of the resulting spurious carrier signal and the I-channel and Q-channel BSPK signals. The actual OQPSK symbols on the phasor diagram are the vector sum of these three components and are shown in Fig. 2(b).

The nonlinear RF amplifier operated at saturation can be modeled as a bandpass hard limiter [4], which is assumed to be ideal with the hard limiter clipping its input signal at levels of $\pm\sqrt{2P_1}(\pi/4)$ and the bandpass filter removing all the harmonics but the one at the carrier frequency. By using Eq. (A-1) in the Appendix, it is easily shown that the resulting bandpass hard-limited OQPSK signal is a constant-envelope signal in the form of

$$\hat{S}_o(t) = \sqrt{2P_1}\cos\left[\omega_c t + \theta_d(t)\right] \tag{4}$$

where $P_1 = P(\beta_1^2 + \gamma_1^2)$ is twice the power actually allocated for the I-channel data modulation and

$$\theta_d(t) = \tan^{-1}\left(\frac{\gamma_1}{\beta_1}\right) - \tan^{-1}\left(\frac{Gm_2\left[t - \dfrac{T_s}{2}\right]\cos\Delta\theta + A\cos\psi}{m_1(t) + Gm_2\left[t - \dfrac{T_s}{2}\right]\sin\Delta\theta + A\sin\psi}\right) \tag{5}$$

is the OQPSK symbol phase profile[3] with

$$\left.\begin{aligned} G &= \sqrt{\frac{\beta_2^2 + \gamma_2^2}{\beta_1^2 + \gamma_1^2}} \\ A &= \sqrt{\frac{(\alpha_1 - \gamma_2)^2 + (\alpha_2 + \delta_1)^2}{\beta_1^2 + \gamma_1^2}} \\ \Delta\theta &= \tan^{-1}\left(\frac{\gamma_2}{\beta_2}\right) - \tan^{-1}\left(\frac{\gamma_1}{\beta_1}\right) \\ \psi &= \tan^{-1}\left(\frac{\alpha_1 - \gamma_2}{\alpha_2 + \delta_1}\right) - \tan^{-1}\left(\frac{\gamma_1}{\beta_1}\right) \end{aligned}\right\} \tag{6}$$

[3] Equation (5) gives the principal value of the symbol phase at a given time. Adding π to some of these principal values is required to place each symbol correctly into its appropriate quadrant.

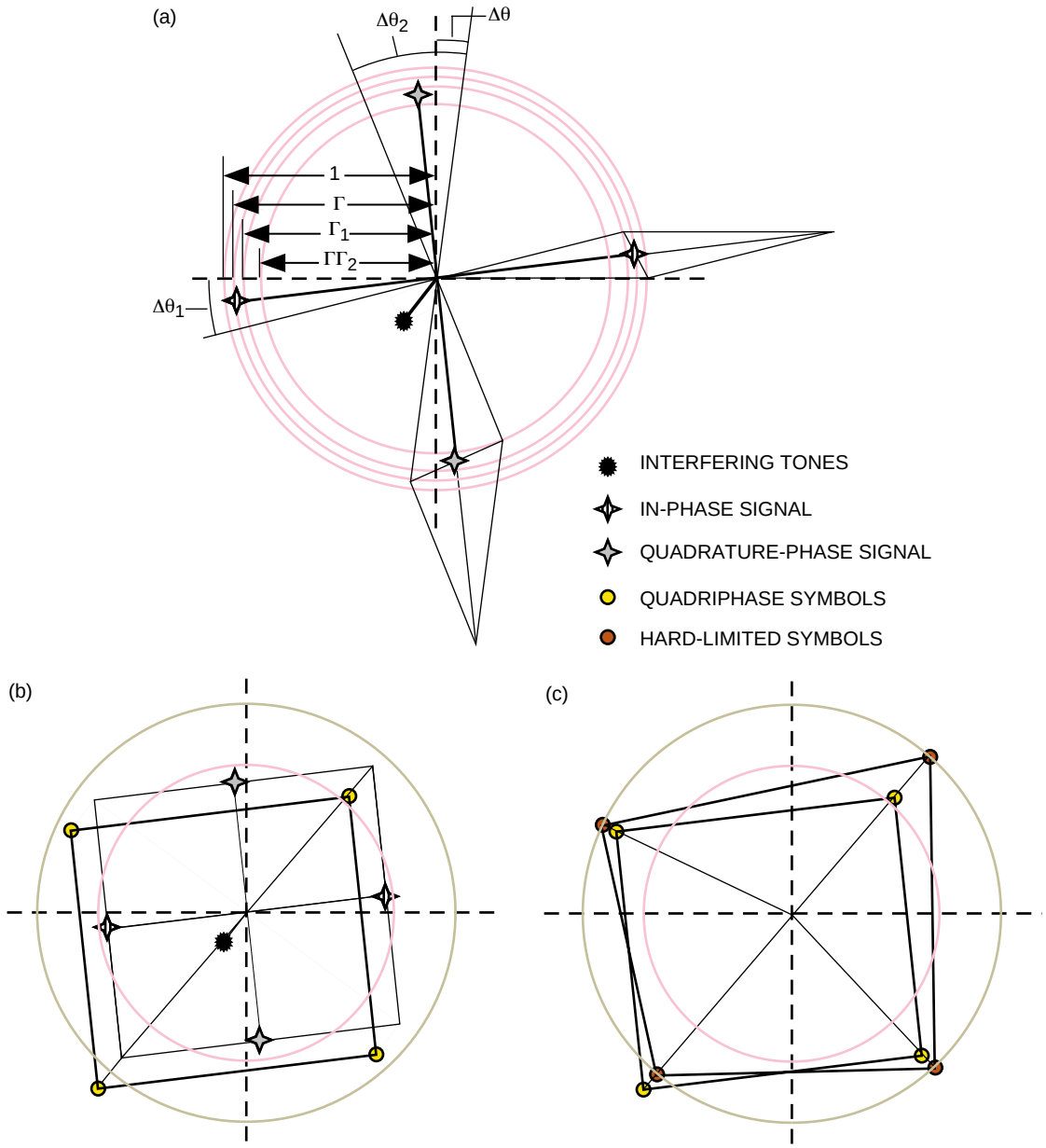

Fig. 2. The phasor diagrams of (a) the individual BPSK signals and the spurious carrier tone signal, (b) the quadriphase symbols for linear channels, and (c) the hard-limited quadriphase symbols for nonlinear channels. (Note that Fig. 2(a) does not have the same scale as the others.)

The four possible values of $\theta_d(t)$, denoted by $\theta_{1,1}$, $\theta_{1,-1}$, $\theta_{-1,-1}$, and $\theta_{-1,1}$, are determined by the data bits as shown in Table 1. Figure 2(c) shows the relationship between the OQPSK symbols on the phasor diagram with and without the hard limiter. The inner and outer circles have radii $\sqrt{P}$ and $\sqrt{2P_1}$, respectively. Note that $P_1 \approx P$ for small modulator imbalances.

The Appendix shows an alternative modulator imbalance model with the commonly specified dc-bias terms in the I- and Q-channels. However, this alternative model is not as flexible as the currently used balanced modulator model. Translations between the two models are included in the appendix.

Table 1. The possible values of $\theta_d(t)$.

$m_1(t)$	$m_2\left(t-\frac{T_s}{2}\right)$	$\theta_d(t)$	Remarks
1	1	$\theta_{1,1}=\tan^{-1}\left(\frac{\gamma_1}{\beta_1}\right)-\tan^{-1}\left(\frac{G\cos\Delta\theta+A\cos\psi}{1+G\sin\Delta\theta+A\sin\psi}\right)$	$\theta_{1,1}\approx-\frac{\pi}{4}$
−1	−1	$\theta_{-1,-1}=\tan^{-1}\left(\frac{\gamma_1}{\beta_1}\right)-\tan^{-1}\left(\frac{G\cos\Delta\theta-A\cos\psi}{1+G\sin\Delta\theta-A\sin\psi}\right)+\pi$	$\theta_{-1,-1}\approx\frac{3\pi}{4}$
1	−1	$\theta_{1,-1}=\tan^{-1}\left(\frac{\gamma_1}{\beta_1}\right)-\tan^{-1}\left(\frac{-G\cos\Delta\theta+A\cos\psi}{1-G\sin\Delta\theta+A\sin\psi}\right)$	$\theta_{1,-1}\approx\frac{\pi}{4}$
−1	1	$\theta_{-1,1}=\tan^{-1}\left(\frac{\gamma_1}{\beta_1}\right)-\tan^{-1}\left(\frac{-G\cos\Delta\theta-A\cos\psi}{1-G\sin\Delta\theta-A\sin\psi}\right)+\pi$	$\theta_{-1,1}\approx\frac{5\pi}{4}$

III. Carrier-Suppression Level

The spurious carrier signal resulting from the modulator imbalances is a signal component that remains constant when data bits change. On the phasor diagram [e.g., see Fig. 2(b)], the spurious carrier signal is the average of all four OQPSK symbol vectors. The square of this vector's length gives the spurious carrier power, which can be put into the form of $(2P_1)\eta$ with

$$\eta=\left(\frac{\cos\theta_{1,1}+\cos\theta_{1,-1}+\cos\theta_{-1,1}+\cos\theta_{-1,-1}}{4}\right)^2+\left(\frac{\sin\theta_{1,1}+\sin\theta_{1,-1}+\sin\theta_{-1,1}+\sin\theta_{-1,-1}}{4}\right)^2 \tag{7}$$

being referred to as the carrier suppression level.

Table 2 lists the carrier-suppression levels calculated for various combinations of worst-case OQPSK modulator imbalances, which are recommended by the CCSDS as 2 deg for phase imbalance and 0.2 dB for amplitude imbalance. The resulting carrier-suppression level actually varies in a range approximately from −34 to −51 dB for these listed cases. This range is about 9-dB lower (or better) than that found in a linear channel.

Table 2. Carrier-suppression levels under various combinations of modulator imbalances (the I/Q power ratio is 0 dB for level-A and 0.4 dB for level-B).

$\Delta\theta$, deg	Γ_1, dB	$\Delta\theta_1$, deg	Γ_2, dB	$\Delta\theta_2$, deg	Carrier suppression level-A, dB	Carrier suppression level-B, dB
0	0	0	0	0	$-\infty$	−331.1330
0	−0.2	2	−0.2	2	−36.8006	−36.4290
0	−0.2	2	0	2	−44.0931	−43.4516
0	0	2	−0.2	2	−36.0347	−35.8117
0	0	2	0	2	−41.1835	−41.1560
0	−0.2	2	−0.2	−2	−34.0511	−34.0458
0	−0.2	2	0	−2	−36.0875	−36.3197
0	0	2	−0.2	−2	−36.0875	−35.8524

Table 2 (contd)

$\Delta\theta$, deg	Γ_1, dB	$\Delta\theta_1$, deg	Γ_2, dB	$\Delta\theta_2$, deg	Carrier suppression level-A, dB	Carrier suppression level-B, dB
0	0	2	0	−2	−41.1835	−41.1546
0	−0.2	−2	−0.2	2	−49.9216	−49.9413
0	−0.2	−2	0	2	−44.4632	−43.8175
0	0	−2	−0.2	2	−44.4632	−45.1554
0	0	−2	0	2	−41.1835	−41.1572
0	−0.2	−2	−0.2	−2	−36.8006	−37.1979
0	−0.2	−2	0	−2	−36.0347	−36.2547
0	0	−2	−0.2	−2	−44.0931	−44.7807
0	0	−2	0	−2	−41.1835	−41.1560
2	−0.2	2	−0.2	2	−36.9909	−36.6216
2	−0.2	2	0	2	−44.4632	−43.8175
2	0	2	−0.2	2	−35.9744	−35.7630
2	0	2	0	2	−41.1835	−41.1572
2	−0.2	2	−0.2	−2	−34.2197	−34.2135
2	−0.2	2	0	−2	−36.1327	−36.3778
2	0	2	−0.2	−2	−36.1327	−35.8849
2	0	2	0	−2	−41.1835	−41.1531
2	−0.2	−2	−0.2	2	−51.1122	−51.1171
2	−0.2	−2	0	2	−44.0931	−43.4516
2	0	−2	−0.2	2	−44.0931	−44.7807
2	0	−2	0	2	−41.1835	−41.1560
2	−0.2	−2	−0.2	−2	−36.9909	−37.3846
2	−0.2	−2	0	−2	−35.9744	−36.1830
2	0	−2	−0.2	−2	−44.4632	−45.1554
2	0	−2	0	−2	−41.1835	−41.1572
−2	−0.2	2	−0.2	2	−36.6055	−36.2313
−2	−0.2	2	0	2	−43.7332	−43.0946
−2	0	2	−0.2	2	−36.0875	−35.8524
−2	0	2	0	2	−41.1835	−41.1546
−2	−0.2	2	−0.2	−2	−33.8801	−33.8757
−2	−0.2	2	0	−2	−36.0347	−36.2547
−2	0	2	−0.2	−2	−36.0347	−35.8117
−2	0	2	0	−2	−41.1835	−41.1560
−2	−0.2	−2	−0.2	2	−48.8385	−48.8668
−2	−0.2	−2	0	2	−44.8441	−44.1932
−2	0	−2	−0.2	2	−44.8441	−45.5423
−2	0	−2	0	2	−41.1835	−41.1583
−2	−0.2	−2	−0.2	−2	−36.6055	−37.0065
−2	−0.2	−2	0	−2	−36.0875	−36.3197
−2	0	−2	−0.2	−2	−43.7332	−44.4178
−2	0	−2	0	−2	−41.1835	−41.1546

IV. Irreducible Carrier-Tracking Error

To track the suppressed carrier of an OQPSK signal by the generalized $IQ(Q^2 - I^2)$-type Costas loop shown in Fig. 3, the received signal, given in Eq. (4), first is mixed with the I-arm and Q-arm reference signals, i.e., $\sqrt{2}\cos(\omega_c t - \phi)$ and $-\sqrt{2}\sin(\omega_c t - \phi)$, with ϕ being the error in the estimated carrier phase. Each of the resulting signals then is passed through an integrate-and-dump (I&D) filter, which is assumed to be driven by a perfectly synchronized symbol-timing clock, rendering the I&D filter outputs

$$\left.\begin{aligned} V_1 &= \frac{\sqrt{P_1}}{2}\left[\cos\left(\theta_d^{(1)} + \phi\right) + \cos\left(\theta_d^{(2)} + \phi\right)\right] + \frac{1}{T_s}\int_0^{T_s} n(t)\sqrt{2}\cos(\omega_c t - \phi)dt \\ V_2 &= \frac{\sqrt{P_1}}{2}\left[\cos\left(\theta_d^{(2)} + \phi\right) + \cos\left(\theta_d^{(3)} + \phi\right)\right] - \frac{1}{T_s}\int_{Ts/2}^{3T_s/2} n(t)\sqrt{2}\sin(\omega_c t - \phi)dt \end{aligned}\right\} \tag{8}$$

where $\theta_d^{(j)}$ is the symbol phase in the interval $(j-1)T_s/2 \le t \le jT_s/2$ and $n(t)$ is a zero-mean white Gaussian noise with a two-sided power spectral density of $N_o/2$ W/Hz. Note that the timings for the I&D filters on the I- and Q-channels are offset by $T_s/2$. Table 3 lists all sixteen possible paths for OQPSK symbol phase transitions in three consecutive $(T_s/2)$ intervals. These paths are equally probable for independent and balanced binary data sources.

The loop-error signal, denoted as Z_o, of the generalized Costas loop is formulated as

$$Z_o = -V_1 V_2 (V_1^2 - V_2^2) \tag{9}$$

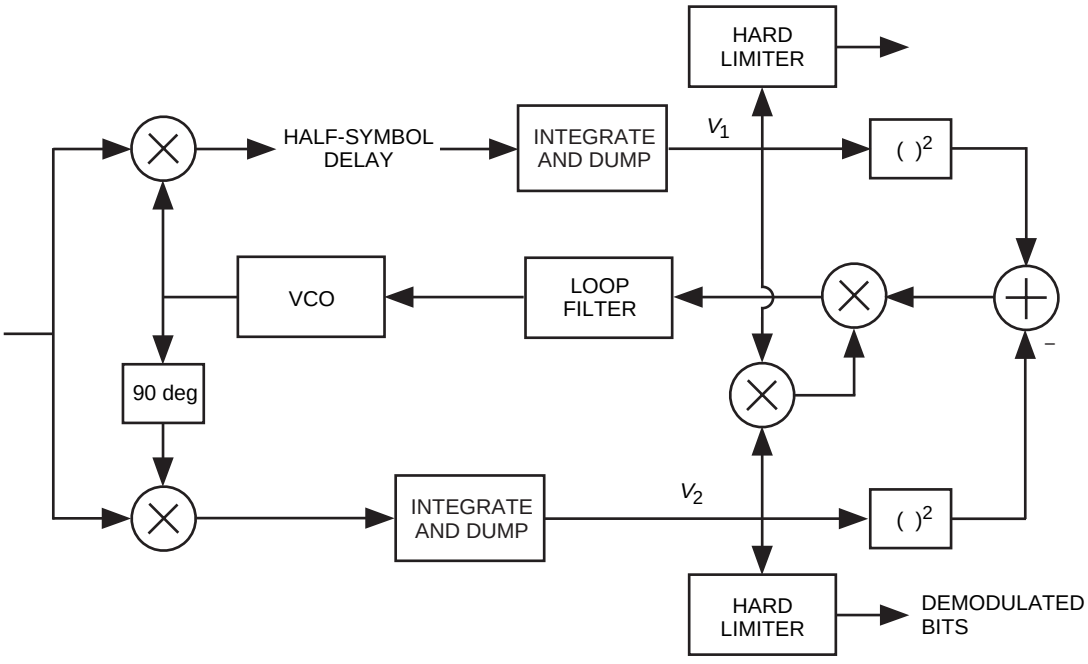

Fig. 3. The generalized Costas loop for OQPSK carrier tracking.

Table 3. All possible paths for OQPSK symbol phase transitions in three consecutive (T_s / 2) intervals.

$\theta_d^{(1)}$	$\longrightarrow$	$\theta_d^{(2)}$	$\longrightarrow$	$\theta_d^{(3)}$
$\theta_{1,1}$	$\longrightarrow$	$\theta_{1,1}$	$\longrightarrow$	$\theta_{1,1}$
				$\theta_{-1,1}$
		$\theta_{1,-1}$	$\longrightarrow$	$\theta_{1,-1}$
				$\theta_{-1,-1}$
$\theta_{-1,-1}$	$\longrightarrow$	$\theta_{-1,-1}$	$\longrightarrow$	$\theta_{-1,-1}$
				$\theta_{1,-1}$
		$\theta_{-1,1}$	$\longrightarrow$	$\theta_{-1,1}$
				$\theta_{1,1}$
$\theta_{1,-1}$	$\longrightarrow$	$\theta_{1,-1}$	$\longrightarrow$	$\theta_{1,-1}$
				$\theta_{-1,-1}$
		$\theta_{1,1}$	$\longrightarrow$	$\theta_{1,1}$
				$\theta_{-1,1}$
$\theta_{-1,1}$	$\longrightarrow$	$\theta_{-1,1}$	$\longrightarrow$	$\theta_{-1,1}$
				$\theta_{1,1}$
		$\theta_{-1,-1}$	$\longrightarrow$	$\theta_{-1,-1}$
				$\theta_{1,-1}$

Carrying out the average of Z_o over the noise and the phase transitions $\theta_d^{(j)}, j = 1, 2, 3$ and equating to zero the averaged error signal, one can solve for the irreducible phase error, denoted as ϕ_o, of this carrier-tracking loop. This irreducible phase error is the negative of the steady-state lock point when the carrier-tracking loop has infinite loop SNR. It turns out that the closed-form solution of such a generalized Costas loop is very involved, including all six arguments (i.e., Γ, Γ_1, Γ_2, $\Delta\theta$, $\Delta\theta_1$, and $\Delta\theta_2$) and, in general, can be solved only numerically.

V. Bit-Error Performance

The error performance is determined by the average BER associated with the demodulated bit streams. It is analyzed by first finding the conditional bit-error probability, $P_b(\phi)$, for a given carrier-tracking error, ϕ, and then averaging it over the probability density function of the phase error, denoted as $p(\phi)$, as characterized by the carrier-tracking loop.

For uncoded OQPSK signals, making hard decisions on V_1 and V_2 in Eq. (8) produces the detected I-channel and Q-channel data bits, respectively. It can be shown that the conditional bit-error probabilities associated with these decisions are

$$P_{b,1}(\phi) = \frac{1}{2}\,\overline{\text{erfc}\left(\frac{1}{2}\sqrt{\frac{P_1 T_s}{N_o}}\left|\cos\left(\theta_d^{(1)}+\phi\right)+\cos\left(\theta_d^{(2)}+\phi\right)\right|\right)}$$

$$= \frac{1}{2}\,\overline{\text{erfc}\left(\sqrt{\frac{2E_b'}{N_o}}\cos\left(\frac{\theta_d^{(1)}-\theta_d^{(2)}}{2}\right)\left|\cos\left(\frac{\theta_d^{(1)}+\theta_d^{(2)}}{2}+\phi\right)\right|\right)} \tag{10a}$$

and

$$P_{b,2}(\phi) = \frac{1}{2}\,\overline{\text{erfc}\left(\frac{1}{2}\sqrt{\frac{P_1 T_s}{N_o}}\left|\sin\left(\theta_d^{(2)}+\phi\right)+\sin\left(\theta_d^{(3)}+\phi\right)\right|\right)}$$

$$= \frac{1}{2}\,\overline{\text{erfc}\left(\sqrt{\frac{2E_b'}{N_o}}\cos\left(\frac{\theta_d^{(2)}-\theta_d^{(3)}}{2}\right)\left|\sin\left(\frac{\theta_d^{(2)}+\theta_d^{(3)}}{2}+\phi\right)\right|\right)} \tag{10b}$$

where the overline denotes the statistical average over the phase transitions $\theta_d^{(j)}, j = 1,2,3$, and $E_b^{'} = (P_1/2)T_s$ is the actual bit energy found in the I-channel data modulation, which differs from the nominal bit energy for each channel, defined as $E_b = (P/2)T_s$, by a factor of $(\beta_1^2 + \gamma_1^2) = P_1/P$. Note that the bit-error probabilities of these two channels are, in general, not identical in the presence of modulator imbalances. The average bit-error probability for OQPSK signals is the arithmetic average of the bit-error probabilities of the I-channel and the Q-channel, given that they both have the same power and bit rate.

By substituting the irreducible phase error, ϕ_o, found for the generalized Costas loop into Eqs. (10a) and (10b), the average bit-error probability and the individual bit-error probabilities for both channels can be evaluated as a function of E_b/N_o for the loop operated at infinite loop SNR, i.e., the case of "perfect" carrier synchronization in which the only phase error remaining is ϕ_o. For realistic scenarios with the loop operated at a finite loop SNR, a Tikhonov distribution centered at ϕ_o is assumed for the carrier-tracking error such that the probability density function of ϕ becomes

$$p(\phi) = \frac{2\exp\left(\rho_{4\phi}\cos\left[4\left(\phi-\phi_o\right)\right]\right)}{\pi I_o(\rho_{4\phi})} \tag{11}$$

where $I_o(\cdot)$ is the modified Bessel function of order zero and

$$\rho_{4\phi} = \frac{1}{\sigma_{4\phi}^2} = \frac{1}{16\sigma_\phi^2} \triangleq \frac{1}{16} \times \text{ (Loop SNR)} \tag{12}$$

By further assuming that the 90-deg phase ambiguity can be perfectly resolved, the average bit-error probability can be evaluated as

$$P_{b,1} = \int_{\phi_o-\pi/4}^{\phi_o+\pi/4} P_{b,1}(\phi)p(\phi)d\phi \tag{13a}$$

and

$$P_{b,2} = \int_{\phi_o-\pi/4}^{\phi_o+\pi/4} P_{b,2}(\phi)p(\phi)d\phi \tag{13b}$$

where $P_{b,1}$ and $P_{b,2}$ are associated with the I-channel and the Q-channel, respectively, and $p(\phi)$ is given in Eq. (11).

To illustrate the worst-case scenario, the following performance comparisons are all based upon the assumption that the actual power in the Q-channel is 0.4-dB less than that in the I-channel or, equivalently, the amplitude imbalance $\Gamma = -0.2$ dB. Tables 4 and 5 list the average and individual bit-error probabilities, under the assumption of perfect carrier synchronization, for the possible combinations within the range constrained by the maximum amplitude imbalance of 0.2 dB and the maximum phase imbalance of 2 deg, when the nominal bit SNRs, E_b/N_o, are 4 dB and 10 dB, respectively. The corresponding irreducible carrier-tracking errors also are included in these tables. Comparing these with the results obtained for a linear channel, it is interesting to note that the relative bit-error performance between the I-channel and the Q-channel is more balanced for all cases listed here, e.g., the largest ratios are about 1.22 and 2.13 here versus 1.48 and 4.80 in a linear channel when the bit SNRs are 4 dB and 10 dB, respectively. This observation is supported by the illustration in Fig. 2(c), of which a more balanced symbol constellation is found in the nonlinear channel than in the linear one. Another interesting observation from these tables is that the average bit-error probabilities are more consistent for all cases listed here, e.g., they are distributed within 15 and 75 percent from the listed reference case when the bit SNRs are 4 dB and 10 dB, respectively. They also are much closer to that of a perfectly balanced OQPSK system[4] than those found in a linear channel.

The best and the worst combinations[5] for these bit-error probabilities as functions of E_b/N_o are plotted in Fig. 4 for the case of perfect carrier synchronization (i.e., with infinite carrier-tracking loop SNR) and in Fig. 5 for the case of imperfect carrier synchronization when the loop SNR is fixed at 22 dB.

Table 4. OQPSK bit-error performance under various combinations of modulator imbalances (E_b/N_o = 4 dB, I/Q power ratio = 0.4 dB, and perfect carrier synchronization).

$\Delta\theta$, deg	Γ_1, dB	$\Delta\theta_1$, deg	Γ_2, dB	$\Delta\theta_2$, deg	$P_b - Avg$ at $E_b/N_0 = 4$ dB	$P_b - I$ at $E_b/N_0 = 4$ dB	$P_b - Q$ at $E_b/N_0 = 4$ dB	ϕ_0, deg	Remarks
0	0	0	0	0	1.2568×10^{-2}	1.1731×10^{-2}	1.3406×10^{-2}	0.0000	Reference
0	−0.2	2	−0.2	2	1.4373×10^{-2}	1.3436×10^{-2}	1.5311×10^{-2}	−0.9789	
0	−0.2	2	0	2	1.4271×10^{-2}	1.3805×10^{-2}	1.4736×10^{-2}	−0.9886	
0	0	2	−0.2	2	1.2731×10^{-2}	1.1451×10^{-2}	1.4010×10^{-2}	−0.9820	(3)
0	0	2	0	2	1.2599×10^{-2}	1.1759×10^{-2}	1.3439×10^{-2}	−0.9978	(1)
0	−0.2	2	−0.2	−2	1.4419×10^{-2}	1.3491×10^{-2}	1.5346×10^{-2}	−0.0563	(2)
0	−0.2	2	0	−2	1.4322×10^{-2}	1.3869×10^{-2}	1.4774×10^{-2}	−0.0133	
0	0	2	−0.2	−2	1.2730×10^{-2}	1.1450×10^{-2}	1.4010×10^{-2}	−0.0871	(3)
0	0	2	0	−2	1.2599×10^{-2}	1.1758×10^{-2}	1.3440×10^{-2}	−0.0482	(1)
0	−0.2	−2	−0.2	2	1.4315×10^{-2}	1.3398×10^{-2}	1.5231×10^{-2}	0.0447	
0	−0.2	−2	0	2	1.4270×10^{-2}	1.3804×10^{-2}	1.4735×10^{-2}	0.0120	
0	0	−2	−0.2	2	1.2671×10^{-2}	1.1415×10^{-2}	1.3927×10^{-2}	0.0801	(3)
0	0	−2	0	2	1.2599×10^{-2}	1.1758×10^{-2}	1.3440×10^{-2}	0.0439	(1)

(1) Cases with the best average bit-error performance.

(2) Cases with the worst average bit-error performance.

(3) Cases with highly unbalanced individual bit-error performances.

[4] The bit-error probabilities for the perfectly balanced OQPSK system are 1.2501×10^{-2} and 3.8721×10^{-6} at an E_b/N_o of 4 dB and 10 dB, respectively.

[5] The combinations corresponding to these extreme cases are different for linear and nonlinear channels.

Table 4 (contd)

$\Delta\theta$, deg	Γ_1, dB	$\Delta\theta_1$, deg	Γ_2, dB	$\Delta\theta_2$, deg	$P_b - Avg$ at $E_b/N_0 = 4$ dB	$P_b - I$ at $E_b/N_0 = 4$ dB	$P_b - Q$ at $E_b/N_0 = 4$ dB	ϕ_0, deg	Remarks
0	−0.2	−2	−0.2	−2	1.4363×10^{-2}	1.3458×10^{-2}	1.5268×10^{-2}	0.9757	
0	−0.2	−2	0	−2	1.4323×10^{-2}	1.3870×10^{-2}	1.4775×10^{-2}	0.9907	
0	0	−2	−0.2	−2	1.2671×10^{-2}	1.1416×10^{-2}	1.3926×10^{-2}	0.9885	(3)
0	0	−2	0	−2	1.2599×10^{-2}	1.1759×10^{-2}	1.3439×10^{-2}	1.0022	(1)
2	−0.2	2	−0.2	2	1.4371×10^{-2}	1.3433×10^{-2}	1.5308×10^{-2}	−2.0254	
2	−0.2	2	0	2	1.4270×10^{-2}	1.3804×10^{-2}	1.4735×10^{-2}	−2.0120	
2	0	2	−0.2	2	1.2731×10^{-2}	1.1452×10^{-2}	1.4011×10^{-2}	−2.0511	(3)
2	0	2	0	2	1.2599×10^{-2}	1.1758×10^{-2}	1.3440×10^{-2}	−2.0439	(1)
2	−0.2	2	−0.2	−2	1.4415×10^{-2}	1.3486×10^{-2}	1.5344×10^{-2}	−1.1021	(2)
2	−0.2	2	0	−2	1.4321×10^{-2}	1.3868×10^{-2}	1.4774×10^{-2}	−1.0358	
2	0	2	−0.2	−2	1.2730×10^{-2}	1.1447×10^{-2}	1.4013×10^{-2}	−1.1564	(3)
2	0	2	0	−2	1.2599×10^{-2}	1.1757×10^{-2}	1.3442×10^{-2}	−1.0944	(1)
2	−0.2	−2	−0.2	2	1.4314×10^{-2}	1.3398×10^{-2}	1.5229×10^{-2}	−1.0013	
2	−0.2	−2	0	2	1.4271×10^{-2}	1.3805×10^{-2}	1.4736×10^{-2}	−1.0114	
2	0	−2	−0.2	2	1.2671×10^{-2}	1.1416×10^{-2}	1.3926×10^{-2}	−0.9885	(3)
2	0	−2	0	2	1.2599×10^{-2}	1.1759×10^{-2}	1.3439×10^{-2}	−1.0022	(1)
2	−0.2	−2	−0.2	−2	1.4361×10^{-2}	1.3455×10^{-2}	1.5267×10^{-2}	−0.0694	
2	−0.2	−2	0	−2	1.4324×10^{-2}	1.3871×10^{-2}	1.4777×10^{-2}	−0.0318	
2	0	−2	−0.2	−2	1.2671×10^{-2}	1.1415×10^{-2}	1.3927×10^{-2}	−0.0801	(3)
2	0	−2	0	−2	1.2599×10^{-2}	1.1758×10^{-2}	1.3440×10^{-2}	−0.0439	(1)
−2	−0.2	2	−0.2	2	1.4376×10^{-2}	1.3437×10^{-2}	1.5316×10^{-2}	0.0677	
−2	−0.2	2	0	2	1.4272×10^{-2}	1.3806×10^{-2}	1.4738×10^{-2}	0.0348	
−2	0	2	−0.2	2	1.2730×10^{-2}	1.1450×10^{-2}	1.4010×10^{-2}	0.0871	(3)
−2	0	2	0	2	1.2599×10^{-2}	1.1758×10^{-2}	1.3440×10^{-2}	0.0482	(1)
−2	−0.2	2	−0.2	−2	1.4423×10^{-2}	1.3496×10^{-2}	1.5350×10^{-2}	0.9894	(2)
−2	−0.2	2	0	−2	1.4323×10^{-2}	1.3870×10^{-2}	1.4775×10^{-2}	1.0093	
−2	0	2	−0.2	−2	1.2731×10^{-2}	1.1451×10^{-2}	1.4010×10^{-2}	0.9820	(3)
−2	0	2	0	−2	1.2599×10^{-2}	1.1759×10^{-2}	1.3439×10^{-2}	0.9978	(1)
−2	−0.2	−2	−0.2	2	1.4316×10^{-2}	1.3398×10^{-2}	1.5233×10^{-2}	1.0907	
−2	−0.2	−2	0	2	1.4269×10^{-2}	1.3803×10^{-2}	1.4735×10^{-2}	1.0354	
−2	0	−2	−0.2	2	1.2671×10^{-2}	1.1412×10^{-2}	1.3929×10^{-2}	1.1488	(3)
−2	0	−2	0	2	1.2599×10^{-2}	1.1757×10^{-2}	1.3442×10^{-2}	1.0901	(1)
−2	−0.2	−2	−0.2	−2	1.4366×10^{-2}	1.3461×10^{-2}	1.5271×10^{-2}	2.0206	
−2	−0.2	−2	0	−2	1.4322×10^{-2}	1.3869×10^{-2}	1.4774×10^{-2}	2.0133	
−2	0	−2	−0.2	−2	1.2672×10^{-2}	1.1417×10^{-2}	1.3928×10^{-2}	2.0571	(3)
−2	0	−2	0	−2	1.2599×10^{-2}	1.1758×10^{-2}	1.3440×10^{-2}	2.0482	(1)

(1) Cases with the best average bit-error performance.

(2) Cases with the worst average bit-error performance.

(3) Cases with highly unbalanced individual bit-error performances.

Table 5. OQPSK bit-error performance under various combinations of modulator imbalances (E_b/N_o = 10 dB, I/Q power ratio = 0.4 dB, and perfect carrier synchronization).

$\Delta\theta$, deg	Γ_1, dB	$\Delta\theta_1$, deg	Γ_2, dB	$\Delta\theta_2$, deg	$P_b - Avg$ at $E_b/N_0 = 10$ dB	$P_b - I$ at $E_b/N_0 = 10$ dB	$P_b - Q$ at $E_b/N_0 = 10$ dB	ϕ_0, deg	Remarks
0	0	0	0	0	4.1125×10^{-6}	3.1437×10^{-6}	5.0812×10^{-6}	0.0000	Reference
0	−0.2	2	−0.2	2	6.8729×10^{-6}	5.2351×10^{-6}	8.5108×10^{-6}	−0.9789	
0	−0.2	2	0	2	6.3385×10^{-6}	5.5931×10^{-6}	7.0839×10^{-6}	−0.9886	
0	0	2	−0.2	2	4.7336×10^{-6}	3.0240×10^{-6}	6.4432×10^{-6}	−0.9820	(3)
0	0	2	0	2	4.2022×10^{-6}	3.1975×10^{-6}	5.2069×10^{-6}	−0.9978	(1)
0	−0.2	2	−0.2	−2	7.1372×10^{-6}	5.4125×10^{-6}	8.8618×10^{-6}	−0.0563	(2)
0	−0.2	2	0	−2	6.5976×10^{-6}	5.8218×10^{-6}	7.3734×10^{-6}	−0.0133	
0	0	2	−0.2	−2	4.7312×10^{-6}	3.0221×10^{-6}	6.4404×10^{-6}	−0.0871	(3)
0	0	2	0	−2	4.2026×10^{-6}	3.1972×10^{-6}	5.2080×10^{-6}	−0.0482	(1)
0	−0.2	−2	−0.2	2	6.5559×10^{-6}	5.0723×10^{-6}	8.0396×10^{-6}	0.0447	
0	−0.2	−2	0	2	6.3337×10^{-6}	5.5894×10^{-6}	7.0781×10^{-6}	0.0120	
0	0	−2	−0.2	2	4.4693×10^{-6}	2.9298×10^{-6}	6.0089×10^{-6}	0.0801	
0	0	−2	0	2	4.2025×10^{-6}	3.1972×10^{-6}	5.2079×10^{-6}	0.0439	(1)
0	−0.2	−2	−0.2	−2	6.8185×10^{-6}	5.2517×10^{-6}	8.3853×10^{-6}	0.9757	
0	−0.2	−2	0	−2	6.6026×10^{-6}	5.8257×10^{-6}	7.3795×10^{-6}	0.9907	
0	0	−2	−0.2	−2	4.4718×10^{-6}	2.9316×10^{-6}	6.0119×10^{-6}	0.9885	
0	0	−2	0	−2	4.2022×10^{-6}	3.1975×10^{-6}	5.2069×10^{-6}	1.0022	(1)
2	−0.2	2	−0.2	2	6.8587×10^{-6}	5.2268×10^{-6}	8.4906×10^{-6}	−2.0254	
2	−0.2	2	0	2	6.3337×10^{-6}	5.5894×10^{-6}	7.0781×10^{-6}	−2.0120	
2	0	2	−0.2	2	4.7381×10^{-6}	3.0254×10^{-6}	6.4509×10^{-6}	−2.0511	(3)
2	0	2	0	2	4.2025×10^{-6}	3.1972×10^{-6}	5.2079×10^{-6}	−2.0439	(1)
2	−0.2	2	−0.2	−2	7.1150×10^{-6}	5.3968×10^{-6}	8.8332×10^{-6}	−1.1021	(2)
2	−0.2	2	0	−2	6.5934×10^{-6}	5.8176×10^{-6}	7.3692×10^{-6}	−1.0358	
2	0	2	−0.2	−2	4.7310×10^{-6}	3.0195×10^{-6}	6.4426×10^{-6}	−1.1564	(3)
2	0	2	0	−2	4.2035×10^{-6}	3.1961×10^{-6}	5.2109×10^{-6}	−1.0944	(1)
2	−0.2	−2	−0.2	2	6.5520×10^{-6}	5.0707×10^{-6}	8.0334×10^{-6}	−1.0013	
2	−0.2	−2	0	2	6.3385×10^{-6}	5.5931×10^{-6}	7.0839×10^{-6}	−1.0114	
2	0	−2	−0.2	2	4.4718×10^{-6}	2.9316×10^{-6}	6.0119×10^{-6}	−0.9885	
2	0	−2	0	2	4.2022×10^{-6}	3.1975×10^{-6}	5.2069×10^{-6}	−1.0022	(1)
2	−0.2	−2	−0.2	−2	6.8071×10^{-6}	5.2433×10^{-6}	8.3710×10^{-6}	−0.0694	
2	−0.2	−2	0	−2	6.6084×10^{-6}	5.8294×10^{-6}	7.3875×10^{-6}	−0.0318	
2	0	−2	−0.2	−2	4.4693×10^{-6}	2.9298×10^{-6}	6.0089×10^{-6}	−0.0801	
2	0	−2	0	−2	4.2025×10^{-6}	3.1972×10^{-6}	5.2079×10^{-6}	−0.0439	(1)
−2	−0.2	2	−0.2	2	6.8893×10^{-6}	5.2429×10^{-6}	8.5356×10^{-6}	0.0677	
−2	−0.2	2	0	2	6.3439×10^{-6}	5.5964×10^{-6}	7.0913×10^{-6}	0.0348	
−2	0	2	−0.2	2	4.7312×10^{-6}	3.0221×10^{-6}	6.4404×10^{-6}	0.0871	(3)
−2	0	2	0	2	4.2026×10^{-6}	3.1972×10^{-6}	5.2080×10^{-6}	0.0482	(1)

(1) Cases with the best average bit-error performance.

(2) Cases with the worst average bit-error performance.

(3) Cases with highly unbalanced individual bit-error performances.

Table 5 (contd)

$\Delta\theta$, deg	Γ_1, dB	$\Delta\theta_1$, deg	Γ_2, dB	$\Delta\theta_2$, deg	$P_b - Avg$ at $E_b/N_0 = 10$ dB	$P_b - I$ at $E_b/N_0 = 10$ dB	$P_b - Q$ at $E_b/N_0 = 10$ dB	ϕ_0, deg	Remarks
−2	−0.2	2	−0.2	−2	7.1617×10^{-6}	5.4279×10^{-6}	8.8956×10^{-6}	0.9894	(2)
−2	−0.2	2	0	−2	6.6026×10^{-6}	5.8257×10^{-6}	7.3795×10^{-6}	1.0093	
−2	0	2	−0.2	−2	4.7336×10^{-6}	3.0240×10^{-6}	6.4432×10^{-6}	0.9820	(3)
−2	0	2	0	−2	4.2022×10^{-6}	3.1975×10^{-6}	5.2069×10^{-6}	0.9978	(1)
−2	−0.2	−2	−0.2	2	6.5613×10^{-6}	5.0731×10^{-6}	8.0495×10^{-6}	1.0907	
−2	−0.2	−2	0	2	6.3294×10^{-6}	5.5851×10^{-6}	7.0737×10^{-6}	1.0354	
−2	0	−2	−0.2	2	4.4685×10^{-6}	2.9272×10^{-6}	6.0098×10^{-6}	1.1488	
−2	0	−2	0	2	4.2034×10^{-6}	3.1961×10^{-6}	5.2107×10^{-6}	1.0901	(1)
−2	−0.2	−2	−0.2	−2	6.8317×10^{-6}	5.2596×10^{-6}	8.4038×10^{-6}	2.0206	
−2	−0.2	−2	0	−2	6.5976×10^{-6}	5.8218×10^{-6}	7.3734×10^{-6}	2.0133	
−2	0	−2	−0.2	−2	4.4758×10^{-6}	2.9328×10^{-6}	6.0187×10^{-6}	2.0571	
−2	0	−2	0	−2	4.2026×10^{-6}	3.1972×10^{-6}	5.2080×10^{-6}	2.0482	(1)

(1) Cases with the best average bit-error performance.

(2) Cases with the worst average bit-error performance.

(3) Cases with highly unbalanced individual bit-error performances.

From Fig. 4, a 0.18-dB I-channel and a 0.35-dB Q-channel worst-case E_b/N_o degradation at the bit-error probability of 10^{-4} are shown under the assumption of perfect carrier synchronization for the CCSDS recommendation of maximum permissible phase imbalance of 2 deg and amplitude imbalance of 0.2 dB. The inferior performance in the Q-channel is expected because of its 0.4-dB power deficiency as a result of the assumed interchannel amplitude imbalance. The overall degradation for the averaged performance is 0.25 dB. The actual performance becomes slightly worse when the carrier-tracking loop is operated at a 22-dB loop SNR. Figure 5 shows a 0.20-dB I-channel and a 0.37-dB Q-channel worst-case degradation at the same bit-error probability, and the overall degradation for the averaged performance becomes 0.27 dB in the imperfect carrier synchronization case.

VI. Conclusion

In this article, the combined effect of modulator imbalances and amplifier nonlinearity on the uncoded OQPSK system subject to the additive white Gaussian noise (AWGN) is analyzed. Both carrier-suppression level and BER performance are evaluated. Numerical results and performance comparisons are given for the CCSDS recommended maximum permissible phase imbalance of 2 deg and amplitude imbalance of 0.2 dB. Based on the above analysis, several conclusions can be drawn concerning the impact of modulator imbalances on the OQPSK system performance:

(1) The impact of modulator imbalances is greatly reduced by the use of a fully saturated, nonlinear RF amplifier to generate a constant-envelope signal for transmission.

(2) The maximum permissible phase imbalance of 2 deg and amplitude imbalance of 0.2 dB would be sufficient for a carrier suppression of 34 dB or more in the nonlinear OQPSK link, which is 9-dB more than that found in the linear OQPSK link.

(3) The maximum permissible phase imbalance of 2 deg and amplitude imbalance of 0.2 dB would be sufficient for an overall degradation of 0.27 dB or less at the BER of 10^{-4} for an OQPSK carrier-tracking loop operated at a reasonable loop SNR of 22 dB or higher. This degradation figure is approximately 0.6-dB better than that found in the linear OQPSK link.

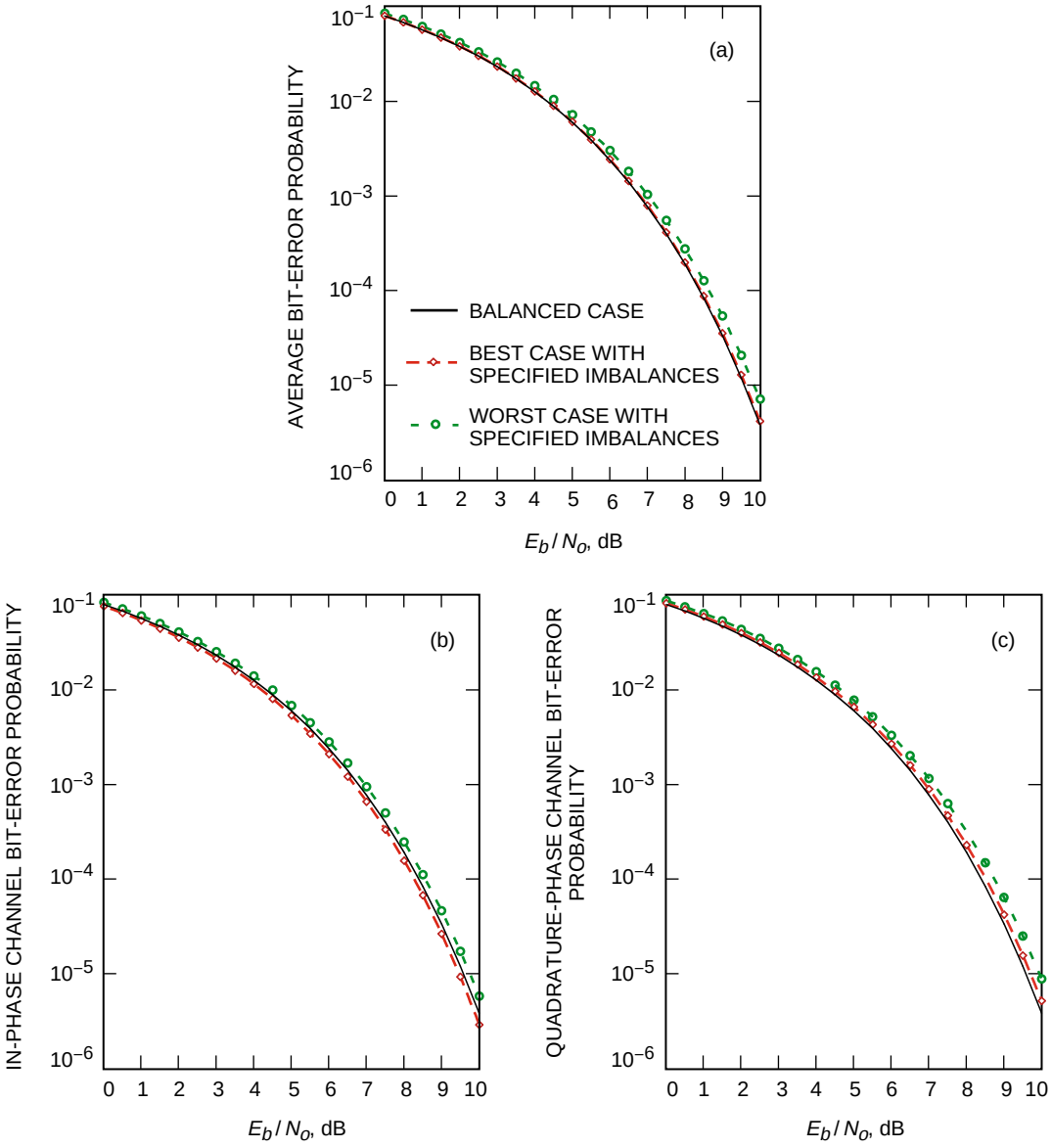

Fig. 4. Bit-error performance of nonlinear OQPSK links with perfect carrier synchronization: (a) overall channel, (b) in-phase channel, and (c) quadrature-phase channel.

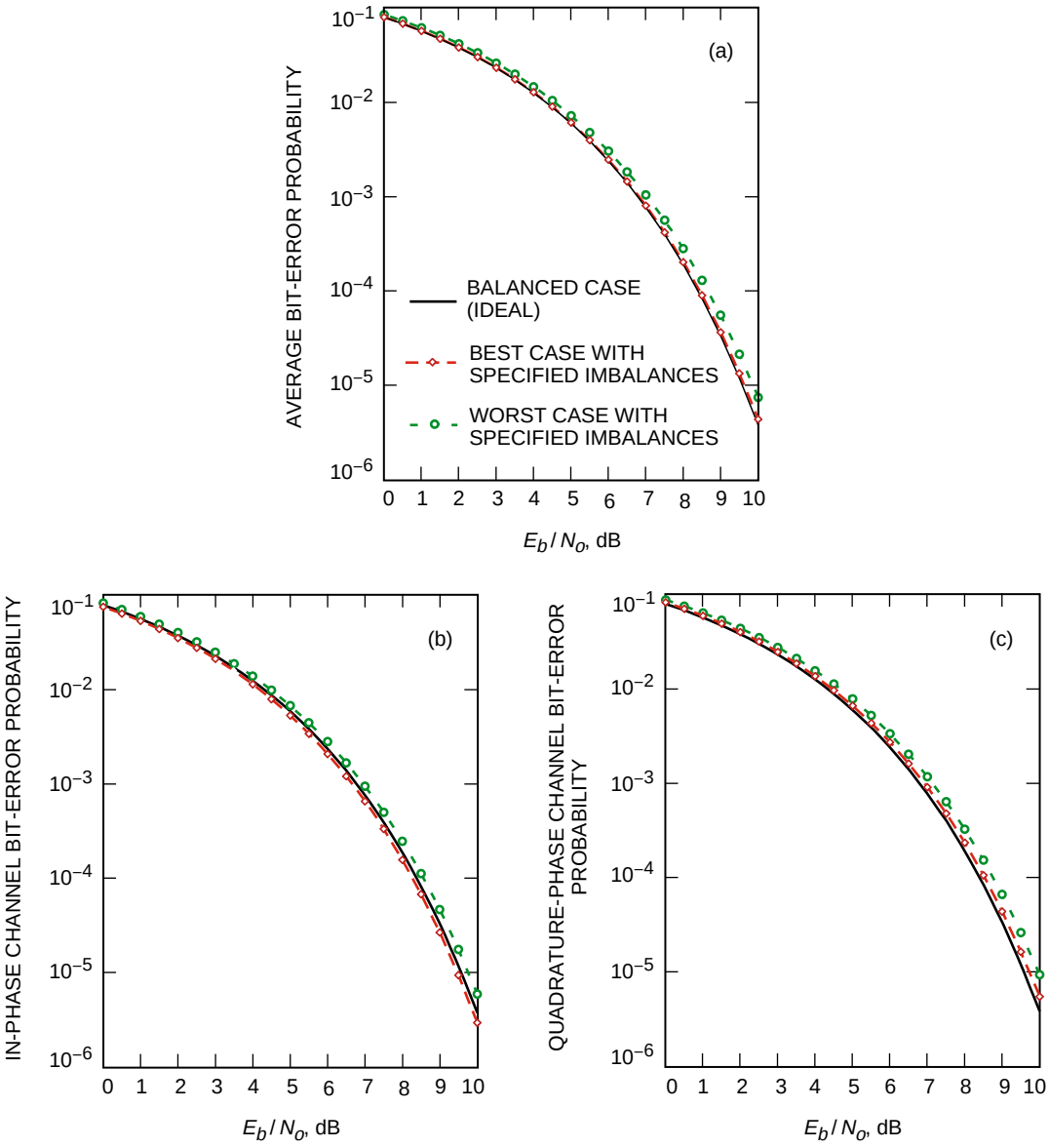

Fig. 5. Bit-error performance of nonlinear OQPSK links with imperfect carrier synchronization (i.e., with a carrier-tracking loop SNR fixed at 22 dB): (a) overall channel, (b) in-phase channel, and (c) quadrature-phase channel.

Acknowledgments

The author would like to thank Dr. Marvin Simon and Dr. Tsun-Yee Yan for their valuable suggestions on this work.

References

[1] H. Tsou, "The Effect of Phase and Amplitude Imbalance on the Performance of Offset Quadrature Phase-Shift-Keyed (OQPSK) Communication Systems," *The Telecommunications and Mission Operations Progress Report 42-135, July–September 1998*, Jet Propulsion Laboratory, Pasadena, California, pp. 1–15, November 15, 1998.
http://tmo.jpl.nasa.gov/tmo/progress_report/42-135/135I.pdf

[2] B. A. Carlson, *Communication Systems*, 2nd. edition, New York: McGraw-Hill, 1975.

[3] Consultative Committee for Space Data Systems, *Recommendations for Space Data System Standards: Radio Frequency and Modulation Systems, Part 1, Earth Stations and Spacecraft*, CCSDS 401.0-B, Blue Book, November 1994.

[4] W. B. Davenport, Jr., and W. L. Root, *An Introduction to the Theory of Random Signals and Noise*, New York: McGraw-Hill, 1958.

Appendix

Alternative OQPSK Modulator Imbalances Models

In this appendix, alternate models of OQPSK modulator imbalances are presented to meet different hardware measurement requirements. The translation of these alternative modulator imbalance models from and to the balanced modulator model used in this article can be established from the equations provided here.

The OQPSK signal from the imperfect balanced modulator, shown in Eq. (1), can be expressed in the following alternate format as

$$S_o(t) = \sqrt{P_1}m_1(t)\cos(\omega_c t + \theta_o) + G\sqrt{P_1}m_2\left(t - \frac{T_s}{2}\right)\sin(\omega_c t + \theta_o + \Delta\theta)$$

$$+ \sqrt{P_1}A\sin(\omega_c t + \theta_o + \psi) \qquad \text{(A-1)}$$

of which the new parameters are related to the parameters used in the balanced modulator model, as given in Eq. (3), by

$$\left.\begin{aligned} P_1 &= P(\beta_1^2 + \gamma_1^2) \\ G &= \sqrt{\frac{\beta_2^2 + \gamma_2^2}{\beta_1^2 + \gamma_1^2}} \\ A &= \sqrt{\frac{(\alpha_1 - \gamma_2)^2 + (\alpha_2 + \delta_1)^2}{\beta_1^2 + \gamma_1^2}} \\ \theta_o &= \tan^{-1}\left(\frac{\gamma_1}{\beta_1}\right) \\ \Delta\theta &= \tan^{-1}\left(\frac{\gamma_2}{\beta_2}\right) - \tan^{-1}\left(\frac{\gamma_1}{\beta_1}\right) \\ \psi &= \tan^{-1}\left(\frac{\alpha_1 - \gamma_2}{\alpha_2 + \delta_1}\right) - \tan^{-1}\left(\frac{\gamma_1}{\beta_1}\right) \end{aligned}\right\} \tag{A-2}$$

where G is the interchannel amplitude imbalance, $\Delta\theta$ is the interchannel phase imbalance, and A and ψ are the amplitude and phase of the spurious carrier, respectively, for this generic model of modulator imbalances.

For modulator imbalances solely attributed to dc-bias terms associated with the individual BPSK signals, the imperfectly modulated OQPSK signal becomes

$$S_o(t) = \sqrt{P_1}[m_1(t) + a_1]\cos\omega_c t + G\sqrt{P_1}\left[m_2\left(t - \frac{T_s}{2}\right) + a_2\right]\sin(\omega_c t + \Delta\theta) \tag{A-3}$$

where a_1 and a_2 are dc-bias terms in the I- and Q-channel signals, respectively. It easily is seen that Eq. (A-3) is related to Eq. (A-1) by

$$A = \sqrt{a_1^2 + G^2 a_2^2 + 2G a_1 a_2 \sin\Delta\theta} \tag{A-4}$$

$$\psi = \tan^{-1}\left(\frac{a_1 + G a_2 \sin\Delta\theta}{G a_2 \cos\Delta\theta}\right) \tag{A-5}$$

Note that this model specifically puts the spurious carrier component in each channel to be in phase with the modulated signal in the same channel. This implicit assumption does not appear in the balanced modulator model.